Transparent anomalous dispersion and superluminal light-pulse propagation at a negative group velocity

A. Dogariu, A. Kuzmich, and L. J. Wang
NEC Research Institute, 4 Independence Way, Princeton, New Jersey 08540
(Received 27 September 2000; published 12 April 2001)

Anomalous dispersion cannot occur in a transparent passive medium where electromagnetic radiation is being absorbed at all frequencies, as pointed out by Landau and Lifshitz. Here we show, both theoretically and experimentally, that transparent linear anomalous dispersion can occur when a gain doublet is present. Therefore, a superluminal light-pulse propagation can be observed even at a negative group velocity through a transparent medium with almost no pulse distortion. Consequently, a *negative transit time* is experimentally observed resulting in the peak of the incident light pulse to exit the medium even before entering it. This counterintuitive effect is a direct result of the *rephasing* process owing to the wave nature of light and is not at odds with either causality or Einstein's theory of special relativity.

DOI: 10.1103/PhysRevA.63.053806 PACS number(s): 42.50.Ct, 03.65.Sq, 42.25.Hz

I. INTRODUCTION

In a seminal paper, Lord Rayleigh remarked that a pulse of light travels at the ''group velocity'' instead of the phase velocity inside a medium [1]. In subsequent papers, Lord Rayleigh further developed the theory on transparency and opacity, and the theory of anomalous dispersion [2,3]. Anomalous dispersion was first studied for mechanical oscillators [3] and was later applied by Sommerfeld and Brillouin [4] to light propagating in absorptive materials. They showed theoretically that inside an absorption line, the dispersion is anomalous, resulting in a group velocity faster than c, the vacuum speed of light. Such an anomalous velocity appears owing to the wave nature of light [5,6].

This, however, raised difficulties with the theory of relativity which states that no velocity can be higher than c, the velocity of light in a vacuum. Brillouin [4] pointed out the following: ''Group velocity, as originally defined, became larger than c or even negative within an absorption band. Such a contradiction had to be resolved and was extensively discussed in many meetings about 1910.''

In order to reconcile the superluminal group velocity in an anomalous dispersion medium with the implied limitation from relativity, Sommerfeld and Brillouin pointed out that causality only requires the speed of a signal carried by light be limited by c, rather than the light pulse itself which travels at the group velocity [4]. They further pointed out that the correct definition of the speed of a light signal should be defined as the ''frontal velocity,'' instead of the somewhat misleadingly named ''signal velocity,'' defined as the speed of the half-point of the front edge of a light pulse. A frontal velocity marks the velocity of an infinitely sharp step-function-like change in the light intensity, albeit even in principle such an infinitely sharp change in time requires infinite bandwidth and thus becomes impractical. It was shown that since the infinitely sharp ''front'' contains an infinitely large bandwidth, a good portion of the power would exceed any practical resonant and nonresonant (plasma) frequencies to have an effective refractive index of unity. Thus this portion of the power will propagate exactly at c to exit the medium at the earliest time and form ''precursors'' [4]. It was an ingenious argument that resolved the apparent conflict of special relativity and superluminal group velocities.

More recently, it has been considered [7–11,13–27] to use various schemes, including the anomalous dispersion near an absorption line [8–11], nonlinear [13] and linear gain lines [14–19,22–24], active plasma medium [17,21], or in a tunneling barrier [25,26] to observe these effects. Sometimes these schemes are applied [9–11,25,26] to observe superluminal propagation of light pulses. Inside an absorption line, it was shown that a light pulse propagates at group velocities faster than c and can become negative with dramatic values of $-c/23{,}000$ [9–12]. However, in all experiments light pulses experienced either very large absorption [9,10] or severe reshaping [25] that sometimes resulted in controversies over the interpretations.

In a series of papers [7,18–20,22–26], Chiao and coworkers showed theoretically that anomalous dispersion can occur inside a transparent material, particularly on the dc side of a single gain line. It was predicted that by using a gain doublet [22], it is possible to obtain a transparent anomalous dispersion region where the group velocity of a light pulse exceeds c with almost no pulse distortion.

Here we use gain-assisted linear anomalous dispersion to demonstrate superluminal light-pulse propagation with a negative group velocity through a transparent atomic medium [27]. We place two Raman gain peaks closely to obtain an essentially lossless anomalous dispersion region that results in a superluminal group velocity. The group velocity of a pulse in this region exceeds c and can even become negative [22,23], while the shape of the pulse is preserved. We measured a negative group velocity index of $n_g = -315(\pm 5)$. Experimentally, a light pulse propagating through the atomic vapor cell exits from it earlier than propagating through the same distance in vacuum by a time difference that is 315 times of the vacuum light propagation time $L/c = 0.2$ ns. Thus, the peak of the pulse exits the cell before it even enters. This counterintuitive effect is a consequence of the wave nature of light and can be well explained

invoking the rephasing process in an anomalously dispersive medium. The observed superluminal light pulse propagation is not at odds with causality, being a direct consequence of classical interference between its different frequency components in an anomalous dispersion region.

II. THEORY OF TRANSPARENT ANOMALOUS DISPERSION

For all transparent matter at a thermal equilibrium such that it is absorptive at all frequencies in the electromagnetic spectrum, the medium's optical dispersion is normal [6]. In other words, for transparent media, the optical refractive index always increases when the frequency of the optical excitation increases. Particularly, Landau and Lifshitz showed that under the condition

$$\mathrm{Im}[\chi(\nu)]\geqslant 0 \quad \text{for any} \quad \nu \tag{1}$$

and in the special case for media with a magnetic permeability $\mu(\nu)=1$, two inequalities hold simultaneously,

$$n_g(\nu)=\frac{d[n(\nu)\nu]}{d\nu}>n(\nu)$$

and

$$n_g(\nu)=\frac{d[n(\nu)\nu]}{d\nu}>\frac{1}{n(\nu)}. \tag{2}$$

Here n_g is the group velocity index: $v_g=c/n_g$, where v_g is the group velocity.

In the case of dielectric media, when an incident light wave's frequency is below the band gap where the media are transparent, the refractive index $n(\nu)>1$. Hence, the group index $n_g>n>1$, resulting in normal dispersion and the group velocity of light pulses slower than c. On the other hand, in the case of metals when the incident light's frequency is higher than the plasma frequency ν_P, the metal becomes transparent with a refractive index $n(\nu)<1$. In this case, the second inequality in Eq. (2) becomes more strict and results in $n_g>1/n>1$. Therefore, the group velocity of a light pulse propagating through metal is also slower than c, the vacuum speed of light.

These conditions are direct results of the Kramers-Kronig relations. Hence, for media in a passive state under Eq. (1) where electromagnetic radiation at all frequencies is transformed into heat and subsequently dissipated, anomalous dispersion and transparency cannot occur simultaneously in the same frequency region.

However, for media with gain, the general assumption in Eq. (1) no longer holds. In a gain medium such as that of an electronic amplifier (e.g., an operational amplifier) or an optical amplifier commonly used for lasers, the imaginary part of the electric susceptibility $\chi(\nu)$ can become negative over a narrow frequency region where gain occurs. Hence, the general results of the inequalities (2) no longer apply and anomalous dispersion can happen in a transparent media, resulting in superluminal group velocities that can even become negative.

A. Classical theory of negative group velocity

In a transparent medium where absorption is negligible, the optical dispersion is primarily governed by its refractive index and the dispersion relation can be written

$$k(\nu)=2\pi\frac{n(\nu)\nu}{c}, \tag{3}$$

where $k(\nu)$ is the wave number for the wave component of frequency ν. The group velocity is hence given by

$$v_g=\frac{c}{n_g}=\mathrm{Re}\left[\frac{d\omega}{dk}\right]=\frac{c}{\mathrm{Re}[n+\nu dn/d\nu]}\approx\frac{c}{n+\nu dn/d\nu}, \tag{4}$$

where

$$n_g=n+\nu\frac{dn}{d\nu} \tag{5}$$

is the group velocity index. In all transparent media where dispersion is normal, we have $dn/d\nu\geqslant 0$, resulting in $v_g\leqslant c$. In special cases where this normal dispersion is very steep over a narrow frequency region such as in the case of electromagnetically induced transparency (EIT) [28,29] that $\nu dn/d\nu\gg 1$, the group velocity can be reduced to as slow as 8 m/sec [30–32,12].

Conversely, in a region of transparent anomalous dispersion where $\nu dn/d\nu\ll -1$, a negative group velocity index is obtained. If the index of refraction decreases rapidly enough with frequency, the group velocity becomes negative. Of course, it is well known that inside an absorption line the refractive index takes a steep drop [4], resulting in an ''anomalous dispersion'' and consequently a negative group velocity [9]. However, the associated heavy absorption that results in opacity makes it difficult to study these effects.

The earlier work of Chiao and co-workers [7,18,22] predicted that it is possible to study steep anomalous dispersion and negative group velocity in a transparent medium where gain rather than absorption occurs at the frequency regions of interest. It is important to have a transparent medium where the majority of the electromagnetic radiation energy is kept in the light fields rather than being dissipated inside the medium via absorption.

Let us start by considering a classical Lorentz oscillator model of the refractive index. The electric displacement is given by

$$D=\varepsilon_0 E+P=\varepsilon_0(1+\chi)E=\varepsilon_0 E(1+N\alpha), \tag{6}$$

where N is the atomic density and α is the atomic polarizability. The polarization density $P=-\varepsilon_0 Nex=\varepsilon_0 N\alpha E$ can be obtained using a simple Lorentz model.

In order to obtain the dipole polarization $p=-ex$ for a bound charge with an intrinsic angular frequency $\omega_0=2\pi\nu_0$ and an angular damping rate $\Gamma=4\pi\gamma$, we start from the equation of motion of the electron,

$$\ddot{x}+\Gamma\dot{x}+\omega_0^2 x=-\frac{eE}{m}=-\frac{eE_0}{m}e^{-i\omega t}. \tag{7}$$

Hence, we obtain

$$x=\frac{eE}{m}\frac{1}{\omega^2-\omega_0^2+i\omega\Gamma}\approx\frac{eE}{2m\omega_0}\frac{1}{\omega-\omega_0+i\Gamma/2}, \tag{8}$$

where the approximation is good as long as $\omega_0\gg\Gamma$. We further obtain for the polarizability,

$$\alpha=-\frac{e^2}{2m\omega_0}\frac{1}{\omega-\omega_0+i\Gamma/2}=-\frac{e^2}{4\pi m\omega_0}\times\frac{1}{\nu-\nu_0+i\gamma}. \tag{9}$$

The dielectric susceptibility of the medium thus can be written

$$\chi(\nu)=-\frac{Ne^2}{4\pi\varepsilon_0 m\omega_0}\times\frac{1}{\nu-\nu_0+i\gamma}=-f\times\frac{M}{\nu-\nu_0+i\gamma}, \tag{10}$$

where $M=\nu_P^2/\nu_0$ with ν_P being the effective plasma frequency and f being the oscillator strength. When two absorption lines are placed nearby with equal oscillator strengths $f_1=f_2=1$, the dielectric susceptibility can be written as

$$\chi(\nu)=-\frac{M}{\nu-\nu_1+i\gamma}-\frac{M}{\nu-\nu_2+i\gamma}. \tag{11}$$

For a narrow frequency region in the middle between the two absorption lines, a steep normal dispersion region occurs, resulting in an ultraslow group velocity [31,32,12].

Conversely, for gain lines, a negative oscillator strength $f=-1$ is assigned [18]. Hence between two closely placed gain lines, the effective dielectric constant can be obtained,

$$\epsilon(\nu)=1+\chi(\nu)=1+\frac{M}{\nu-\nu_1+i\gamma}+\frac{M}{\nu-\nu_2+i\gamma}. \tag{12}$$

For a dilute gaseous medium, we obtain from Eq. (12) for the refractive index $n(\nu)=n'(\nu)+in''(\nu)=1+\chi(\nu)/2$ and the real and imaginary parts of the refractive index are plotted in Fig. 1. It is evident from Fig. 1 that a steep anomalous dispersion region appears without the heavy absorption present. In fact, a residual gain persists. Furthermore, with the correct choice of experimental parameters, the steep drop of the refractive index as a function of frequency can be made a mostly linear one in this region. Thus a light pulse with a frequency bandwidth within this narrow linear anomalous dispersion region will experience almost no change in pulse shape upon propagating through such a medium.

Now, we consider the propagation of a light pulse of an arbitrary shape through a transparent anomalous dispersing medium of a length L as illustrated in Fig. 2. For a scalar light pulse that is decomposed into its positive and negative frequency parts,

$$E(z,t)=E^{(+)}(z,t)+E^{(-)}(z,t), \tag{13}$$

we have for its Fourier decomposition

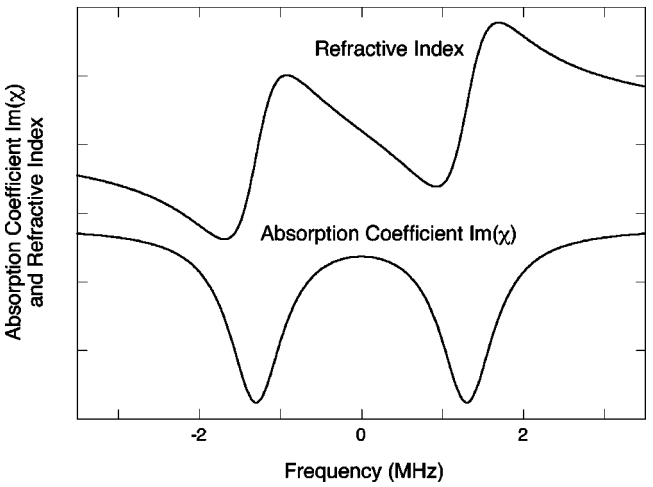

FIG. 1. Gain-assisted anomalous dispersion. Figure shows frequency-dependent gain coefficient and refractive index.

$$E^{(+)}(z,t)=\frac{1}{\sqrt{2\pi}}\int d\omega\tilde{E}^{(+)}(\omega)e^{-i(\omega t-k\cdot z)}. \tag{14}$$

At the entrance of the medium where we denote by $z=0$, we can rewrite the above expression as

$$E^{(+)}(0,t)=\frac{1}{\sqrt{2\pi}}e^{-i\omega_0 t}\int d(\omega-\omega_0)\tilde{E}^{(+)}(\omega-\omega_0)\times e^{-i(\omega-\omega_0)t}, \tag{15}$$

where ω_0 is the carrier frequency of the light pulse. Inside the transparent anomalous dispersion medium, if over the narrow bandwidth of the incident light pulse $\tilde{E}(\omega-\omega_0)$, the gain is essentially unity, the propagation is governed by the wave vector $k(\omega)$. Using a Taylor-series expansion of the wave vector,

$$k(\omega)=k(\omega_0)+\frac{1}{v_g}(\omega-\omega_0)+\frac{1}{2}\frac{d^2k}{d\omega^2}\bigg|_{\omega_0}(\omega-\omega_0)^2, \tag{16}$$

where the expansion is carried to the quadratic term. Nonlinear terms in the expansion of Eq. (16) are often associated with ''group velocity dispersion (GVD),'' or chirping terms causing pulse distortion. When these nonlinear terms in Eq.

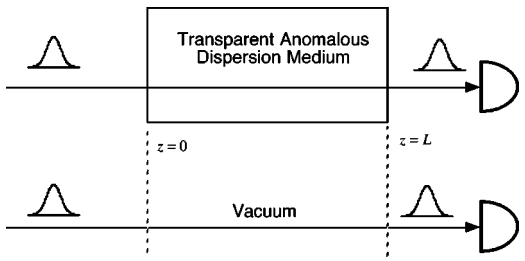

FIG. 2. Pulse propagation through a medium of a length L and a group velocity index $v_g=c/(n+\nu dn/d\nu)$. Pulse propagation through the same length in vacuum is also shown for comparison.

(16) are negligible, i.e., the dispersion is essentially linear, from Eqs. (14) and (16) we obtain

$$E^{(+)}(L,t)=\frac{1}{\sqrt{2\pi}}e^{-i(\omega_0 t-k_0 L)}\int d(\omega-\omega_0)\tilde{E}^{(+)}(\omega-\omega_0)\times e^{-i(\omega-\omega_0)(t-L/v_g)}. \quad (17)$$

Hence, the intensity of the light pulse as a function of time measured with a detector (shown in Fig. 2), $I(L,t)$, is related to the incident pulse's time-dependent intensity by

$$I(L,t)=\frac{\varepsilon_0 cA}{2}|E^{(+)}(L,t)|^2=\frac{\varepsilon_0 cA}{2}|E(0,t-L/v_g)|^2=I(0,t-L/v_g), \quad (18)$$

where A is the beam area.

Ordinarily, in a normal dispersion medium, the group velocity $v_g<c$. Hence, the output intensity of a pulse propagating through the medium is retarded by the propagation time L/v_g, resulting in a delay longer than the vacuum transit time L/c. In a transparent anomalous dispersion medium, the group velocity $v_g=c/[n+\nu dn/d\nu]$ can exceed c provided the anomalous dispersion is sufficiently strong such that $n+\nu dn/d\nu<1$. In this case, the group velocity becomes superluminal: $v_g>c$, resulting in a ''*superluminal transit time*:'' $L/v_g<L/c$, the vacuum transit time. Hence the output pulse's time-varying profile is related to the input pulse by a delay that is shorter than the vacuum transit time L/c resulting in a superluminal propagation of the light pulse.

Furthermore, when the transparent anomalous dispersion becomes stronger to yield $n+\nu dn/d\nu=0$, the group velocity $v_g=c/[n+\nu dn/d\nu]$ approaches infinity, resulting in a ''*zero transit time*,'' such that Eq. (18) gives $I(L,t)=I(0,t-L/v_g)=I(0,t)$. In this case, the output pulse and the input pulse vary the same way in time and there is no time delay experienced by the pulse propagating through the medium that has a length of L.

Finally, when the transparent anomalous dispersion becomes very steep, such as for the case illustrated in Fig. 1, the dispersive term $\nu dn/d\nu$, which is negative, becomes very large in its magnitude such that $|\nu dn/d\nu|\gg 1$, resulting in a negative group velocity $v_g=c/[n+\nu dn/d\nu]<0$. In this case, Eq. (18) gives $I(L,t)=I(0,t+|L/v_g|)$, where the quantity $|L/v_g|=|n_g|L/c$ is positive and can become very large compared to the vacuum transit time L/c. This means that the intensity at the output of the medium of length L, $I(L,t)$, will vary in time *earlier* than that of the input pulse $I(0,t)$. Thus in this case, a ''*negative transit time*'' can be observed. The time difference between the output pulse and the input pulse in the form of the pulse advance that is $|n_g|$ fold of the vacuum transit time L/c. Practically, since the shape of the pulse is not changed, this results in a rather counterintuitive phenomenon where a certain part of the light pulse has already exited the medium before the corresponding part of the incident light pulse even enters by a time difference that is $|n_g|$ times of the vacuum transit time L/c.

This rather counterintuitive effect is a result of the wave nature of light.

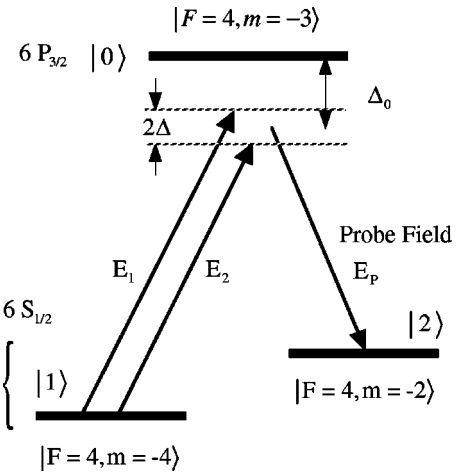

FIG. 3. Schematic atomic level diagram.

B. Quantum theory of atomic response in transparent anomalous dispersion

In order to correctly model the electromagnetic responses of a dilute atomic gaseous medium, one must compute its dielectric susceptibility using the quantum-mechanical treatment. In this section we provide a simplified yet realistic model of a transparent anomalous dispersion medium realized using two Raman gain lines in a Λ system shown in Fig. 3.

In a simplified Λ system, two continuous-wave (cw) Raman pump light fields are present for the creation of the gain doublet shown in Fig. 1. The two Raman pump fields are different in frequency by a small amount $2\Delta\nu$. For simplicity, we will first ignore the Doppler shift and assume that the atoms are at rest.

We begin by treating the simple case of a single Raman pump field and compute the linear dielectric susceptibility for the Raman probe field. Let us first suppose that all atoms are initially prepared in an energy ground state $|1\rangle$ via optical pumping. In the atomic system, another ground state $|2\rangle$ is also present and a Raman transition from $|1\rangle$ to $|2\rangle$ can take place via an off-resonance two-photon transition through an excited state $|0\rangle$ by absorbing a pump photon and emitting a probe photon, with a corresponding transition from the state $|1\rangle$ to $|2\rangle$. The effective Hamiltonian for such a Λ system coupled with the Raman pump and probe fields can be written as

$$\hat{H}=\hat{H}_0+\hat{H}_I, \quad (19)$$

where

$$\hat{H}_0=-\hbar\omega_{01}|1\rangle\langle 1|-\hbar\omega_{02}|2\rangle\langle 2|, \quad (20)$$

with $\omega_{0j}=(E_0-E_j)/\hbar$ for $j=1,2$. The interaction Hamiltonian can be written as

$$\hat{H}_I = -\hbar\Omega_1 e^{-i\omega_1 t}|0\rangle\langle 1| - \hbar\Omega_2 e^{-i\omega_2 t}|0\rangle\langle 2| + \text{H.c.}, \tag{21}$$

where $\Omega_j = (\hat{e}_j \cdot \vec{\mu}_{0j})E_j/2\hbar$ $(j=1,2)$ is the Rabi frequency for the pump and the probe fields, respectively. $\vec{\mu}_{0j}$ is the dipole moment between the states $|j\rangle$ and the excited state $|0\rangle$. Because E_1 is a strong Raman pump field while E_2 is a weak Raman probe field, we therefore have $|\Omega_1| \gg |\Omega_2|$.

Without involving a complicated density operator treatment which is only necessary in a full quantum theory where the electromagnetic field is also quantized, we can apply here a simplified state vector treatment in order to obtain the dielectric susceptibility of a dilute gaseous atomic medium. The state vector of an atom can be written as

$$|\psi(t)\rangle = a_0(t)|0\rangle + a_1(t)e^{i\omega_{01}t}|1\rangle + a_2(t)e^{i\omega_{02}t}|2\rangle. \tag{22}$$

Hence, we obtain for the amplitude of the excited state $|0\rangle$,

$$\dot{a}_0(t) = i\Omega_1 e^{-i\Delta_1 t}a_1 + i\Omega_2 e^{-i\Delta_2 t}a_2, \tag{23}$$

where $\Delta_j = \omega_j - \omega_{0j}$ $(j=1,2)$ represent the detuning of the Raman pump and probe beams, respectively. To the lowest order of approximation, we have for the state amplitudes $a_1 \approx 1$ and $a_2 \approx 0$. We further note the fact that the common detuning $\Delta_0 = (\Delta_1 + \Delta_2)/2$ is much greater than the differential detuning $\Delta_1 - \Delta_2$. Under these conditions, we have from Eq. (23)

$$a_0(t) \approx -\frac{\Omega_1}{\Delta_0} e^{-i\Delta_1 t}a_1. \tag{24}$$

Note here that we have omitted the decay of the excited-state amplitude a_0 in Eq. (23). First, the broadened linewidth is still much narrower than the common detuning Δ_0 such that Eq. (24) is a good approximation. Second, in a Raman scheme as used in the experiment the major factor of the Raman transition broadening is due to transit time broadening rather than the effective excited-state decay rate: $(\Omega_1^2/\Delta_0^2)/T_2$, where T_2 is the excited-state lifetime. Hence, Eq. (24) is a good approximation.

Next we obtain the equation of motion for the amplitude of the Raman final state $|2\rangle$

$$\dot{a}_2(t) = -i\frac{\Omega_1\Omega_2^*}{\Delta_0} e^{-i(\Delta_1-\Delta_2)t}a_1 - \Gamma a_2. \tag{25}$$

Here a phenomenological decay rate Γ is used to account for the Raman transition line broadening. Solving Eq. (25), we obtain

$$a_2(t) = \left(\frac{\Omega_1\Omega_2^*}{\Delta_0}\right)\frac{1}{(\Delta_1-\Delta_2)+i\Gamma} e^{-i(\Delta_1-\Delta_2)t}a_1. \tag{26}$$

Using Eqs. (24) and (26) and the definition of the dielectric polarization $P = N\mu_{2,0}\rho_{02} = \chi\varepsilon_0 E_2$ where the density-matrix element $\rho_{02} = a_0 a_2^* e^{-i\omega_{02}t}$ and N being the atomic density, we obtain for the dielectric susceptibility for the Raman probe field E_2,

$$\chi(\Delta_2) = -N\frac{|\mu_{02}\hat{e}_2|^2}{2\hbar\varepsilon_0}\frac{|\Omega_1|^2}{\Delta_0^2}\frac{1}{(\Delta_1-\Delta_2)-i\Gamma}. \tag{27}$$

Using the fact that $\Delta_1 - \Delta_2 = -2\pi[\nu_2 - (\nu_1 - \nu_{01} + \nu_{02})]$, and redefining $\nu_0 = (\nu_1 - \nu_{01} + \nu_{02})$ while replacing ν_2 with ν, we can rewrite Eq. (27) as

$$\chi(\nu) = \frac{M}{\nu - \nu_0 + i\gamma}, \tag{28}$$

where the factor

$$M = N\frac{|\mu_{02}\hat{e}_2|^2}{4\pi\hbar\varepsilon_0}\frac{|\Omega_1|^2}{\Delta_0^2}. \tag{29}$$

When two Raman pump beams of equal strengths and slightly different frequencies $\nu_0 - \Delta\nu$ and $\nu_0 + \Delta\nu$ are present, the dielectric susceptibility of the Raman probe field becomes

$$\chi(\nu) = \frac{M}{(\nu - \nu_0 - \Delta\nu) + i\gamma} + \frac{M}{(\nu - \nu_0 + \Delta\nu) + i\gamma}, \tag{30}$$

similar to that obtained using a classical Lorentz model given in Eq. (11).

However, in a gaseous atomic medium, there is Doppler broadening that demands the expressions in Eqs. (29) and (30) being modified. Specifically, the common detuning in Eq. (29), Δ_0, needs to be replaced by the shifted detuning $\Delta_0 + \nu_0 V/c$, where ν_0 is the carrier frequency of the light field and V is the velocity of those atoms in a specific velocity group $G(V)$ for which the atoms move along the light propagation direction with a speed V. Owing to the colinear propagation geometry, the Doppler shifts in both Δ_1 and Δ_2 are essentially the same. Hence, the shifts in frequencies in $\Delta_1 - \Delta_2$ or $\nu - \nu_0 \pm \Delta\nu$ are essentially zero to within an error of $\Delta\nu V/c$ which is negligible. Therefore, Eq. (30) needs only be modified by replacing the expression of the M factor with

$$M = N\frac{|\mu_{02}\cdot\hat{e_2}|^2}{4\pi\hbar\varepsilon_0}\int dV \frac{|\Omega_1|^2}{(\Delta_0 + \nu V/c)^2}G(V). \tag{31}$$

The effects of this modification are twofold. First, the quadratic dependence on $1/(\Delta_0 + \nu V/c)^2$ in Eq. (31) is an even function which prevents cancellation of the effect due to Doppler broadening. This is a direct result of using Raman transitions. Second, for some velocity groups V_0, the shifted detuning $\Delta_0 + \nu V_0/c$ may vanish. However, for these velocity groups the Raman pump beams act like reversed optical pumping which empties these velocity groups such that $G(V_0) = 0$. This is similar to the ''spectral hole burning'' effect commonly known in laser physics. Furthermore, the atoms reversely pumped away in these velocity groups act like a broadband weak absorber that helps to compensate the residual gain as shown in Fig. 1.

The spectral linewidths of the gain lines are approximately given by

$$\gamma \approx \frac{v_R}{2\pi w_0}, \tag{32}$$

due to transit broadening [33]. Here v_R is the mean atomic velocity in the radial direction and w_0 is the mean radius of the Gaussian beam.

C. Parameter dependence in Gaussian pulse propagation

The primary result of Eq. (18), $I(L,t)=I(0,t-L/v_g)$, applies to light pulses of arbitrary shapes, provided that over the pulse bandwidths the dispersion is transparent and linear. In order to further examine the implications and limits of pulse propagation in a transparent anomalous dispersion medium, here we treat the propagation of a Gaussian pulse.

For the propagation of a Gaussian pulse through a transparent anomalous dispersion medium, there are three important parameters: the peak intensity, the pulse advancement, and the pulse shape distortion. In this section we calculate the parameter dependence of these factors on various experimental parameters. These parameter dependencies will be compared with experimental results.

To begin, let us refer to Fig. 2 and consider a Gaussian pulse of a temporal duration τ and an angular carrier frequency ω_0, for which the incident wave form becomes

$$E(z,t)=E_0 e^{-(t-z/c)^2/2\tau^2} e^{-i\omega_0(t-z/c)} \quad (z<0). \tag{33}$$

At the entrance of a transparent anomalous dispersion medium $z=0$, the electric field hence varies in time as

$$E(0,t)=E_0 e^{-t^2/2\tau^2} e^{-i\omega_0 t}. \tag{34}$$

Therefore, at the exit surface of a medium of length L, the electric field varies in time

$$E(L,t)=\frac{\tau E_0 e^{-\eta L}}{\sqrt{2\pi}}\int e^{-\tau^2(\omega-\omega_0)^2/2} e^{-i(\omega_0 t-kL)} d\omega$$
$$=\alpha E_0 e^{-\beta^2(t-L/v_g)^2/2\tau^2} e^{-i\omega_0[t-n'(\omega_0)L/c]}, \tag{35}$$

where

$$\alpha = e^{-n''(\omega_0)\omega_0 L/c-\eta L}\beta = e^{gL}\beta \tag{36}$$

describes the change in pulse amplitude due to residual amplification and a weak broadband absorption factor η, resulting in a phenomenological gain coefficient gL. The change in the width of the pulse is entirely characterized by the parameter

$$\beta=\left[1-i\frac{L}{\tau^2}\frac{d^2k}{d\omega^2}\bigg|_{\omega_0}\right]^{-1/2}. \tag{37}$$

Using the simple expression in Eqs. (30) and (31), here we calculate the scaling dependence of various quantities that can be compared with experimental results. First, using Eq. (30), we obtain a residual gain coefficient of

$$g=-n''(\omega_0)\omega_0/c-\eta=\frac{2\pi\nu_0 M}{c}\frac{\gamma}{(\Delta\nu^2+\gamma^2)}-\eta. \tag{38}$$

We note here that the factor M is linear in the atomic density N and the Raman pump beam power $|\Omega_1|^2$ as given in Eq. (31). Meanwhile, the residual loss coefficient η, which is due to the absorption of atoms reversely pumped away into other atomic states is also linear in the atomic density N. Its dependence on the Raman pump power is more complex since power broadening and common detuning are involved.

Next, we calculate the pulse advance (negative delay) ΔT for a Gaussian pulse propagating through an anomalous dispersion medium of length L. Referring to the experimental situation illustrated in Fig. 2, a light pulse propagating through a transparent anomalous dispersion medium of a length L is advanced compared to the same pulse propagating through the same distance in a vacuum by

$$\Delta T=(1-n_g)\frac{L}{c}=-\nu_0\frac{dn}{d\nu}\bigg|_{\nu_0}\frac{L}{c}. \tag{39}$$

Using the expression in Eq. (30), we have for the pulse advance

$$\Delta T=\nu_0 M\frac{L}{c}\frac{\Delta\nu^2-\gamma^2}{(\Delta\nu^2+\gamma^2)^2}. \tag{40}$$

The pulse propagating through the transparent anomalous dispersion medium is advanced provided that $\Delta\nu>\gamma$. Here we further note that the pulse advance, ΔT, is linear in M which is linear in the atomic density N and the Raman pump power $|\Omega_1|^2$. These parameter dependencies will be compared with experimental results.

Finally, we compute the pulse width change factor β. We notice from Eq. (37) that β depends on the derivative of the group velocity index n_g. From Fig. 1 it is apparent that the frequency-dependent change of the real part of the refractive index $n'(\nu)$ is essentially linear in the narrow frequency region between the two gain lines. It is the imaginary part, i.e., the gain coefficient that appears to have a quadratic change as a function of frequency. Therefore, the majority of the potential change in the width of an incident pulse will be due to the quadratic change in the imaginary part of the refractive index. We obtain using Eq. (30),

$$\frac{d^2k}{d\omega^2}\bigg|_{\omega_0}=-iM\nu_0\frac{\gamma(3\Delta\nu^2-\gamma^2)}{\pi c(\Delta\nu^2+\gamma^2)^3}. \tag{41}$$

Hence, from Eq. (7), the pulse width distortion factor β becomes

$$\beta=\left[1-M\nu_0\frac{L}{\pi c\tau^2}\frac{\gamma(3\Delta\nu^2-\gamma^2)}{(\Delta\nu^2+\gamma^2)^3}\right]^{-1/2}. \tag{42}$$

When various parameters such as the M factor (linear in Raman pump power and atomic density) and the length of the atomic chamber L, are significantly increased, or the pulse duration τ is significantly decreased, the factor β will become reasonably different from (larger than) unity. In these cases, $\beta > 1$ will result in a narrowing in the pulse's temporal width. In the present experiment, this pulse distortion factor β is only 1.002.

III. EXPERIMENTS

From the theoretical treatment above, we see that a variety of parameters have to be taken into consideration in experimentation. From an experimental point of view, one must satisfy the following requirements. First, a gain doublet must be obtained for which the anomalous dispersion between the gain lines can become linear to avoid any pulse distortion. In previous work, excited-state population inversion was considered to obtain gain [22]. However, spontaneous emission and the short excited-state lifetime would cause such gain doublets to be very difficult to sustain. It is important to have a steady-state gain with a lifetime longer than the pulse duration τ to avoid transient effects and the associated complications. Second, the medium must be transparent since opaque anomalous dispersion has been long known and has resulted in controversies in terms of interpretations. While ideally the dispersion shown in Fig. 1 is transparent, residual absorption and the associated loss are often present and cannot be simply discarded in experimental situations. Third, in order to show superluminal light-pulse propagation in a linear regime, one must employ a very weak light pulse for which the photon number is far less than the atomic number in order to avoid Raman gain saturation. Fourth, in order to achieve a reasonable accuracy in the measurement, a system should be designed to demonstrate a negative group velocity. In this case the pulse advancement under conventional experimental situation will be substantially large compared with commonly obtained accuracy (about 1 ns). A number of other experimental conditions also have to be considered such as atomic density, polarization decay time, etc., and they will be discussed in the following sections as well.

A. Experimental setup

The experiment is performed using an atomic cesium (Cs) vapor cell at 30 °C and the main setup is shown in Fig. 4. The cesium atoms are confined in a 6-cm-long Pyrex glass cell coated with paraffin for the purpose of maintaining atomic ground-state spin polarization. The atomic cell is placed inside a magnetic shield made of a thin layer of high-μ metal material inside which the Earth's magnetic field is reduced to the submilligauss level. A Helmholtz coil (not shown in Fig. 4) produces a uniform magnetic field inside the magnetic shield parallel to the propagation direction of all optical beams. This uniform field is approximately 1 G serving the purpose of defining a quantization axis for optical pumping. Inside the magnetic shield, the air temperature is controlled using a heater servo system in order to control the temperature of the cesium cell. During data acquisition, this control system is turned off to avoid any stray magnetic field. Owing to good thermal insulation, the temperature of the atomic cell remains the same during the data acquisition time.

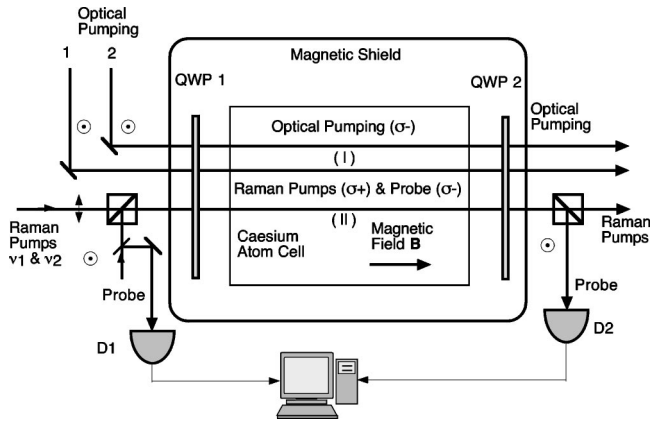

FIG. 4. Schematic experimental setup. Two optical pumping beams tuned to the cesium (Cs) atomic $D1$ and $D2$ transitions prepare the atoms in its ground-state hyperfine sublevel $|F=4,m=-4\rangle$. Two Raman pump beams and a Raman probe beam derived from a common narrow linewidth diode laser propagate colinearly parallel to a small magnetic field B through the atomic cell. Two $\lambda/4$ plates (QWP1 and QWP2) are used to prepare the three light beams into the corresponding circular polarization states and then separate them for analysis.

In region I of Fig. 4 two optical pumping laser beams prepare almost all cesium atoms into the ground-state hyperfine magnetic sublevel $6S_{1/2}$, $|F=4,m=-4\rangle$ that serves as the state $|1\rangle$ in Fig. 3. Laser-1 is a narrow linewidth diode laser locked to the 852-nm D_2 transition of Cs using a Lamb-dip technique and empties the $6S_{1/2}$, $F=3$ hyperfine ground states. Laser-2 is a broadband tunable Ti:sapphire laser tuned to the 894-nm D_1 transition of cesium. The linewidth of laser-2 covers transitions from both the $6S_{1/2}$, $F=4$ and $F=3$ hyperfine ground states to the $6P_{1/2}$ excited state. Both laser beams are initially linear polarized and are turned into left-hand polarization $(\sigma-)$ using a quarter-wave plate placed before the atomic cell. Inside the vapor cell, cesium atoms collide with the paraffin-coated glass walls and the atoms change their velocities inside the Doppler profile. However, their ground-state spin polarizations are not changed during collisions. Hence, all atoms inside the entire Doppler-broadening profile are optically pumped into the ground-state $|F=4,m=-4\rangle$ quickly. The mean dephasing time of the ground state spin polarization of cesium atoms in a paraffin-coated cell is of the order of a fraction of a second.

In region II three light beams derived from the same narrow linewidth diode laser propagate colinearly through the cell. Two strong continuous-wave (cw) Raman pump beams are right-hand polarized $(\sigma+)$ and a weak Raman probe beam is left-hand polarized $(\sigma-)$. Using three acousto-optical modulators (AOM's), the frequency difference of the two Raman pump beams can be tuned continuously over a few MHz while the probe beam can also be tuned in frequency and can be operated in both cw or pulsed mode. The typical carrier frequency of the AOM's is 80 MHz and the

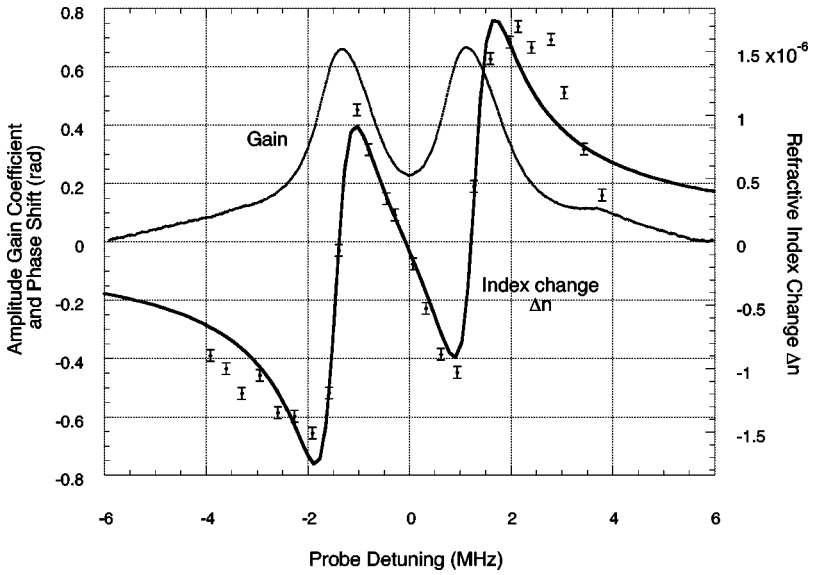

FIG. 5. Measured refractive index and gain coefficient. The superposed curve over the index data is obtained using Eq. (30) with parameters $\nu_0, \Delta\nu$, and γ obtained experimentally.

linewidth is about 20 kHz. A residual optical beam that is shifted in frequency by 80 MHz generated from the same AOM that modulates the probe beam is also available for the refractive index measurement.

B. Experimental methods and results

First we operate the Raman probe beam in a tunable cw mode to measure the gain and refractive index of the atomic system as a function of the probe frequency detuning. Figure 5 shows the measured gain coefficient and the refractive index. In order to obtain the gain coefficient, we first measure the intensity of the transmitted probe beam as a function of probe frequency. We then extract the gain coefficient.

The refractive index is measured using a radio-frequency (rf) interferometric technique. We send two CW light beams from the probe beam input port of the polarized beam splitter. These two optical beams are different in frequency by $\Omega \approx$ 80 MHz (derived from the zeroth- and the first-order output of the probe AOM). A weak probe beam is tuned in frequency to be close to the Raman pump frequency and a strong local oscillator field shifted by $\Omega \approx$ 80 MHz is outside of the interesting frequency range. The rf beating signal is detected using two fast detectors $D1$ and $D2$. We ac couple both output signals and record the beating signal of $D2$,

$$V_{on}(t, \phi_{on}(\nu)) = V_0 \cos[\Omega\,\delta t - \phi_{on}(\nu) - \phi_0], \qquad (43)$$

as a function of the AOM frequency Ω, using the ac-coupled $D1$ voltage signal as the trigger. We then apply a least-squares fitting procedure using Eq. (43) to obtain the frequency-dependent phase shift $\phi_{on}(\nu)$. In Eq. (43), δt is a residual difference between the electrical delays of the trigger channel and the signal channel and is minimized. ϕ_0 is a fixed phase factor. Of course, the fitting procedure always only yields the combined phase shift,

$$\phi_{on}(\nu) - \delta\Omega\,\delta t = 2\pi n(\nu) L/\lambda - \delta\Omega\,\delta t, \qquad (44)$$

where $\delta\Omega = \Omega - \Omega_0$ ($\Omega_0 = 80$ MHz) is the change in frequency relative to the mean carrier frequency. In order to achieve high accuracy of the refractive index measurement, one must separately measure the factor $\delta\Omega\,\delta t$. To do this, we tune the diode laser outside of the Doppler profile where the atoms are irrelevant and Eq. (43) becomes

$$V_{off}(t) = V_1 \cos[\Omega\,\delta t - \phi_{off} - \phi_0] \qquad (45)$$

since here the phase shift $\phi_{off} = 0$. Hence, we directly measure the factor $\delta\Omega\,\delta t$ and can subtract it out from the combined phase shift in Eq. (44) to obtain the refractive phase shift to obtain the refractive index: $\phi_{on}(\nu) = 2\pi n(\nu) L/\lambda$. The result is shown in Fig. 5. The superimposed curve is obtained from Eq. (30) using parameters obtained from the gain measurement. From Fig. 5 we readily see that a negative change of $\Delta n = -1.8 \times 10^{-6}$ in the refractive index occurs over a narrow probe frequency range of $\Delta\nu = 1.9$ MHz between the two gain lines. Using the expression of the group-velocity index, we obtain the result $n_g = -330(\pm 30)$ in that frequency region. The 10% error reflects the accuracy of the phase measurement.

Next, a pulsed Raman probe beam is employed to observe the superluminal propagation. A near Gaussian probe pulse with a 2.4 μsec full width at half maximum (FWHM) is generated by applying a biased sinusoidal electronic signal to the probe beam A/O modulator. The repetition rate is 50 kHz. A portion of the pulsed probe beam is divided at a beamsplitter before the atomic cell and aligned onto photodiode $D1$ as a reference. Because the total number of atoms in the probe volume limits the maximum net energy gain of the probe pulse, we use a very weak probe beam ($\approx 1\,\mu$W) in order to avoid saturation and hence to optimize the anomalous dispersion. A high sensitivity avalanche photodiode, reverse-biased below breakdown, serves as detector $D2$ to measure the weak probe pulse that propagates through the atomic cell. The photoelectric current produced by detector $D2$ is converted to a voltage signal using a 500-Ω load resistor and recorded by a digitizing oscilloscope using a syn-

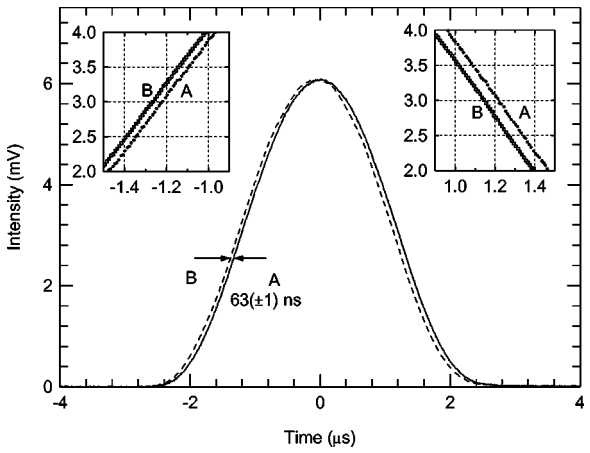

FIG. 6. Measured pulse advancement for a light pulse traversing through the cesium vapor. *A*, light pulse far off resonance from the cesium $D2$ transitions propagating at speed c through 6 cm of vacuum. *B*, same light pulse propagating through the same Cs cell near resonance with a negative group velocity $-c/315$. The insets show the front and trail parts of the pulses. *A* and *B* are both the average of 1000 pulses. Off-resonance pulse *A* is normalized to the magnitude of *B*.

chronized output signal from the pulse generator as the trigger. Pulses from detector $D1$ are also recorded.

In order to measure the pulse propagation time, we first tune the diode laser that produces the Raman pump and probe beams far off-resonance from the 852-nm cesium $D2$ lines (by 2.5 GHz) to measure the time-dependent probe-pulse intensity. When the laser is placed far off resonance, the atoms have no effect and the probe pulse propagates at the speed c inside the cell. We then tune the diode laser back to within the Doppler absorption profile and lock it on its side. Using the same synchronized pulse generator output signal as the trigger, we record the time-dependent probe-pulse intensity measured by detector $D2$. We verify that no systematic drift is present by tuning the laser off resonance again by the same amount and recording the probe-pulse signal; the two off-resonance pulses are identical to within less than 1 ns. Probe pulses both on and off resonance are shown in Fig. 6 (average of approximately 1000 pulses). Curve *A* in Fig. 6 shows the light pulses far off resonance from the cesium $D2$ transitions propagating at speed c through 6 cm of vacuum. Curve *B* shows the same light pulse propagating through the same Cs cell near resonance at a negative group velocity $-c/315$. Probe pulses on resonance show a 40% transmittance and this is due to the broadband absorption by those atoms reverse pumped away from the state $|F=4,m=-4\rangle$. It is evident that there is almost no change in the pulse shape. The front edges and the trailing edges of the pulses are shown in the insets; both edges are shifted forward by the same amount.

Using a least-squares fitting procedure, we obtain a pulse advancement shift of 63 (± 1) nsec. Compared with the 0.2-nsec propagation time for light to traverse the 6-cm length of the atomic cell in vacuum, the 63-nsec advancement gives an effective group index of $n_g=-315(\pm 5)$. This is in good agreement with that inferred from the refractive index measurement. The pulses measured with detector $D1$ are also recorded in the sequence of the off-, on-, off-resonance pulse propagation measurements and are found to be identical to within 1.5 ns.

We note here that the measured superluminal pulse propagation inside the transparent anomalous dispersion medium is a linear effect. We further estimate the photon number per pulse and the interacting atomic number to show that there is no saturation effect present. In the experiment, the measured voltage signal peak strength is $V_p=\alpha\xi RG\dot{N}_{ph}\hbar\omega_0$, where $\alpha\approx 0.5A/W$ is the photo responsivity of the avalanche photo detector and $\xi=0.2$ is the effective efficiency of the detection imaging system. $R=500\,\Omega$ is the load resistance. $G\approx 80$ is the avalanche gain. $\hbar\omega_0=1.5$ eV is the photon energy. Hence, we obtain the peak photon rate $\dot{N}_{ph}\approx 5\times 10^{12}$/sec. Using the 2.4-$\mu$sec FWHM as the pulse duration, each probe pulse contains approximately 1.2×10^7 photons. On the other hand, inside the volume of the probe light beam $\pi w_0^2 L$, there are on average $N\pi w_0^2 L$ atoms at any given moment, where $N\approx 10^{11}$ cm^{-3} is the atomic density. The beam radius is approximately 90 μm and the cesium cell is of a length 6 cm, the number of atoms inside the beam volume is approximately 1.4×10^8 at any given moment. However, since atoms are coming in and out of this volume within an average time of $2w_0/V_R\approx 1$ μsec, during the 2.4-μsec pulse duration there are approximately 3.4×10^8 atoms inside the volume of the light pulse, much larger than the photon number per pulse. Hence, gain saturation effects are insignificant and the observed superluminal pulse propagation is a linear effect.

To further analyze the linearity of the response of the anomalous dispersion medium, we compute the pulse area of the Raman transition $\Omega_R\tau$. Here $\Omega_R=|\Omega_1\Omega_2/\Delta_0|$ is the effective Raman Rabi frequency. By using Eq. (29) and by noting that $\Omega_2=(\vec{\mu}_{02}\cdot\widehat{e_2})E_2/2\hbar$, we obtain

$$M|E_2|^2=N\frac{\hbar}{\pi\varepsilon_0}\left|\frac{\Omega_1\Omega_2}{\Delta_0}\right|^2, \tag{46}$$

where N is the atomic density. Furthermore, we have for the probe electric field E_2, $P_2=2\varepsilon_0 cA|E_2|^2=\dot{N}_{ph}\hbar\omega_0$, where P_2 is the Raman probe power, $A=\pi w_0^2$ is the beam cross section, and $\hbar\omega_0$ is the energy per photon. Hence we obtain from Eq. (46)

$$\left|\frac{\Omega_1\Omega_2}{\Delta_0}\right|^2=\frac{\pi M\omega_0\dot{N}_{ph}}{2NcA}.$$

We further recall from Eq. (28) that the peak Raman gain $G=gL$ at one of the resonances is $G=\pi ML/\gamma\lambda$. Therefore, we obtain for the effective Raman Rabi frequency

$$\Omega_R=\left|\frac{\Omega_1\Omega_2}{\Delta_0}\right|=\sqrt{\frac{\pi G\gamma\dot{N}_{ph}}{N\pi w_0^2 L}}. \tag{47}$$

Using the experimental parameters of $\dot{N}_{ph}=5\times 10^{12}$/sec, $N\pi w_0^2 L=1.4\times 10^8$, peak gain $G=0.7$, and $\gamma=0.45$ MHz,

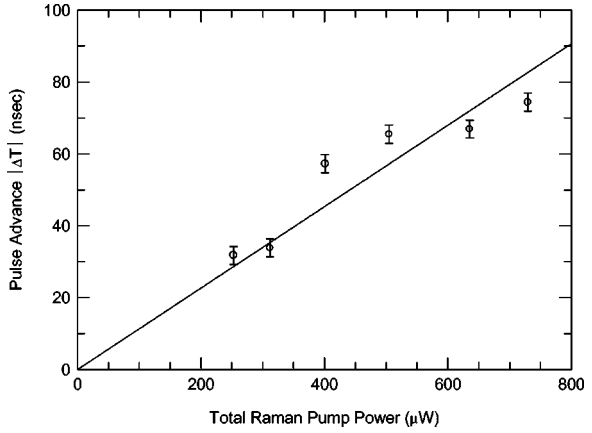

FIG. 7. Measured pulse advance $|\Delta T|$ dependence on total Raman pump power. The solid line shows the least-square fitting based on the linear dependence shown in Eq. (40).

we obtain $\Omega_R = 1.25 \times 10^5$/sec. This is far smaller than the typical Raman detuning $\Delta\nu \approx 1.4$ MHz. Recall that during the 2.4 μsec pulse duration, the average dwell time for the atoms is $\Delta\tau = 2w_0/V_R = 1$ μsec. Hence, the equivalent pulse area becomes $\Omega_R \Delta\tau \approx 0.13$. It is apparent that saturation of Raman gain is negligible.

Next, we perform experiments to test the parameter dependence given by Eq. (40). Namely, the pulse advancement $|\Delta T|$ is linear in the parameter M which depends linearly on the Raman pump power P_R and the atomic density N. First, the pulse advancement ΔT is measured as a function of the total Raman pump power of the two gain lines using the method described above. Figure 7 shows the experimental result. In Fig. 8 we show the measured parameter dependence of pulse advancement $|\Delta T|$ as a function of atomic density. We measure the optical density of the atomic medium in an ancillary linear absorption experiment while varying the temperature of the atomic cell. The optical density of the atomic cell is proportional to the atomic density N.

Finally, we measure the pulse delay/advancement ΔT as a

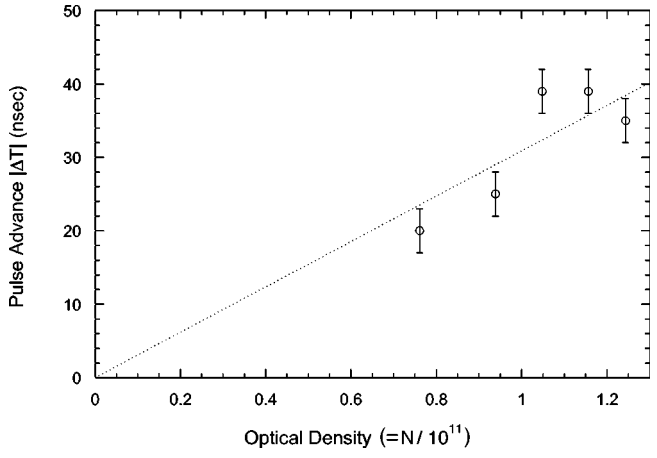

FIG. 8. Measured pulse advance $|\Delta T|$ dependence on the optical density of the Cs chamber (linear in atomic density N). The solid line shows the least-square fitting based on the linear dependence shown in Eq. (40).

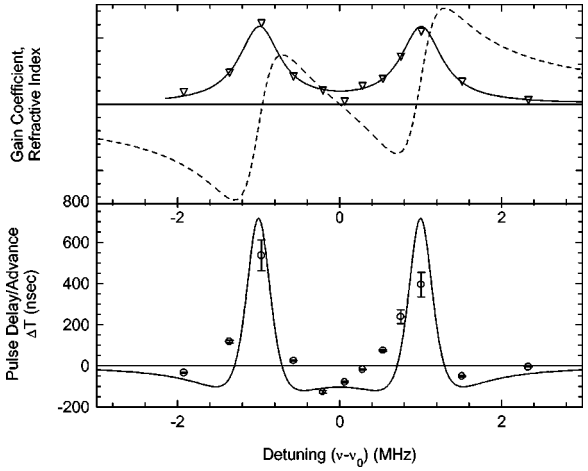

FIG. 9. Measured pulse gain coefficient and pulse delay/advance ΔT as a function of the carrier frequency of the light pulse. The dashed line shows the theoretical curve of the refractive index using parameters extracted from the gain coefficient using Eq. (30). The solid line shows the theoretical value of the pulse advance/delay based on the gain coefficient and refractive index.

function of the pulse carrier frequency ν. Figure 9 shows the measurement results. For several values of the carrier frequency ν, the pulse gain is measured. We further record the pulse forms for the laser frequency tuned off and on resonance. Using the measured pulse gain, we obtain the gain coefficient and fit the data using Eq. (30). Using the fitting parameters, we compute the theoretical value of the refractive index and group delay/advancement plotted also in Fig. 9. The large error bar for the pulse delay measurement near the gain lines is due to the rapid change in group velocity index and gain, causing severe pulse shape distortions. The simple model based on a Lorentz oscillator is in good agreement with the experimental results.

IV. DISCUSSION AND CONCLUSION

As remarked by Lord Rayleigh [1], the group velocity of a light pulse is the result of interference between its various frequency components. Here we note that the measured negative and superluminal group velocity of a light pulse propagating through a transparent anomalous dispersion medium is due to the physical effect of ''rephasing.'' Specifically, inside an anomalous dispersion medium, a longer wavelength (redder) component of a light pulse has a slower phase velocity, contrary to the case of a normal dispersion medium. Conversely, a shorter wavelength component (bluer) has a faster phase velocity. Inside a medium of refractive index n, the effective wavelength of a light ray is modified: $\lambda' = \lambda/n$, where λ is the vacuum wavelength. Therefore, in a sufficiently strong anomalous dispersion medium, the redder incident ray will have a shorter wavelength and hence becomes a bluer ray, while an incident bluer ray will have a longer wavelength to become a redder ray. This results in an unusual situation where the phases of the different frequency components of a pulse become aligned at the exit surface of the medium earlier than even in the case

of the same pulse propagating through the same distance in a vacuum.

This highly unusual circumstance was poorly understood because it only occurred previously in absorption lines. Furthermore, inside an opaque medium, the majority of the incident light energy is absorbed and subsequently dissipated by the medium making it difficult to define the energy velocity of light. In the present experiment, an anomalous dispersion region is created in a transparent medium. Hence it becomes possible to speak about the energy velocity of a light pulse [34,35].

Here we note that the physical mechanism that governs the observed superluminal light propagation has been traditionally viewed as ''virtual'' reshaping [7,20]. In the past, such superluminal light pulse propagation has been widely viewed as the result of the amplification of the pulse's front edge and the absorption of its tail, despite that it had been repeatedly pointed out that such reshaping is actually a ''virtual process'' [7,20]. In the present experiment, the 2.4 μsec (FWHM) probe pulse has only a 160-kHz bandwidth (FWHM) which is much narrower than the 2.7-MHz separation of the two gain lines and the probe pulse is placed in the middle of these gain lines spectrally. Hence, the probe pulse contains essentially no spectral components that are resonant with the Raman gain lines to be amplified. Therefore, the argument that the probe pulse is advanced by amplification of its front edge does not apply. Furthermore, the average time an atom stays inside the volume of the Raman probe beam is less than 1 μsec, shorter than the 2.4 μsec FWHM of the pulse. Hence, even if the atoms are amplifying the probe pulse, both the leading and the trailing edges would be amplified as both edges interact with atoms in the same state. This view is not consistent with the experiment. Hence it is worth emphasizing that the ''reshaping'' of the pulse can be only viewed as ''virtual reshaping'' [7,25] aimed at providing an intuitive understanding. Strictly speaking, the superluminal light propagation observed here is the result only of the anomalous dispersion region created with the assistance of two nearby Raman gain resonances. In other words, it is largely due to the rapid anomalous change of the refractive index as is shown in Eq. (30) rather than the gain. When the gain coefficient becomes large, its effect appears as the compression of the pulse, as indicated by Eqs. (37) and (42). We further stress that the observed superluminal light propagation is a result of the wave nature of light [5]. It can be understood using the classical theory of wave propagation in an anomalous dispersion region where interference between different frequency components produces this rather counterintuitive effect.

ACKNOWLEDGMENTS

We thank R. A. Linke for several stimulating discussions. We thank J. A. Giordmaine, R. Y. Chiao, S. E. Harris, and E. S. Polzik for helpful discussions. We thank E. B. Alexandrov and N. P. Bigelow for the use of the paraffin-coated cesium cell.

[1] Lord Rayleigh, Nature (London) **XXIV**, 382 (1881); also in *Collected Optics Papers of Lord Rayleigh* (Optical Society of America, Washington, DC, 1994), paper No. 75.
[2] Lord Rayleigh, Nature (London) **LX**, 64 (1899).
[3] Lord Rayleigh, Philos. Mag. **XLVIII**, 151 (1899).
[4] L. Brillouin, *Wave Propagation and Group Velocity* (Academic Press, New York, 1960).
[5] M. Born and E. Wolf, *Principles of Optics*, 7th ed. (Cambridge University Press, Cambridge, 1997).
[6] L. D. Landau and E. Lifshitz, *Electrodynamics of Continuous Media* (Pergamon, Oxford, 1960), p. 286.
[7] R. Y. Chiao, in *Amazing Light, a Volume Dedicated to C. H. Townes on His Eightieth Birthday*, edited by R. Y. Chiao (Springer, New York, 1996), p. 91.
[8] C. G. B. Garrett and D. E. McCumber, Phys. Rev. A **1**, 305 (1970).
[9] S. Chu and S. Wong, Phys. Rev. Lett. **48**, 738 (1982).
[10] B. Segard and B. Macke, Phys. Lett. **109A**, 213 (1985).
[11] A. M. Akulshin, S. Barreiro, and A. Lezama, Phys. Rev. Lett. **83**, 4277 (1999).
[12] D. Budker, D. F. Kimball, S. M. Rochester, and V. V. Yashchuk, Phys. Rev. Lett. **83**, 1767 (1999).
[13] N. G. Basov *et al.*, Sov. Phys. JETP **23**, 16 (1966).
[14] L. Casperson and A. Yariv, Phys. Rev. Lett. **26**, 293 (1971).
[15] A. Icsevgi and W. E. Lamb, Phys. Rev. **185**, 517 (1969).
[16] E. Picholle *et al.*, Phys. Rev. Lett. **66**, 1454 (1991).
[17] D. L. Fisher and T. Tajima, Phys. Rev. Lett. **71**, 4338 (1993).
[18] R. Y. Chiao, Phys. Rev. A **48**, R34 (1993).
[19] E. L. Bolda, R. Y. Chiao, and J. C. Garrison, Phys. Rev. A **48**, 3890 (1993).
[20] R. Y. Chiao, J. Boyce, and J. C. Garrison, in *Fundamental Problems in Quantum Theory, in Honor of Professor John A. Wheeler,* edited by D. M. Greenberg and A. Zeilinger, Special issue of Ann. N.Y. Acad. Sci. **755**, 400 (1993).
[21] D. L. Fisher, T. Tajima, M. C. Downer, and C. W. Siders, Phys. Rev. E **51**, 4860 (1995).
[22] A. M. Steinberg and R. Y. Chiao, Phys. Rev. A **49**, 2071 (1994).
[23] M. W. Mitchell and R. Y. Chiao, Am. J. Phys. **66**, 14 (1998).
[24] E. L. Bolda, J. C. Garrison, and R. Y. Chiao, Phys. Rev. A **49**, 2938 (1994).
[25] R. Y. Chiao and A. M. Steinberg, in *Progress in Optics,* edited by E. Wolf (Elsevier, Amsterdam, 1997), p. 345.
[26] A. M. Steinberg, P. G. Kwiat, and R. Y. Chiao, Phys. Rev. Lett. **71**, 708 (1993).
[27] L. J. Wang, A. Kuzmich, and A. Dogariu, Nature (London) **406**, 277 (2000).
[28] S. E. Harris, Phys. Today **50(7)**, 36 (1997).
[29] M. O. Scully and M. S. Zubairy, *Quantum Optics* (Cambridge University Press, Cambridge, 1997).

[30] M. Xiao *et al.*, Phys. Rev. Lett. **74**, 666 (1995).
[31] L. V. Hau, S. E. Harris, Z. Dutton, and C. H. Behroozi, Nature (London) **397**, 594 (1999).
[32] M. M. Kash *et al.*, Phys. Rev. Lett. **82**, 5229 (1999).
[33] J. E. Thomas and W. W. Quivers, Phys. Rev. A **22**, 2115 (1980).
[34] G. Diener, Phys. Lett. A **223**, 327 (1996).
[35] G. Diener, Phys. Lett. A **235**, 118 (1997).